

## Field emission conduction mechanisms in chemical vapor deposited diamond and diamondlike carbon films

Paul W. May<sup>a)</sup> and Stefan Höhn

*School of Chemistry, University of Bristol, Bristol BS8 1TS, United Kingdom*

Wang N. Wang and Neil A. Fox

*Department of Physics, University of Bristol, Bristol BS8 1TR, United Kingdom*

(Received 27 October 1997; accepted for publication 26 February 1998)

Field emission properties of undoped chemical vapor deposited diamond and diamondlike carbon films have been measured for a variety of different deposition conditions. The nature and appearance of the damage site after testing, together with the mathematical form of the observed current–voltage relations, are correlated with the conductivity of the film. This is consistent with a model for the overall current which is a combination of conduction mechanisms through the bulk of the film with Fowler–Nordheim tunneling. © 1998 American Institute of Physics.

[S0003-6951(98)02217-7]

The emission of electrons from the surface of diamond and diamondlike carbon (DLC) films is currently of much interest due to potential applications in cold cathode devices. The negative electron affinity (NEA) of the hydrogenated diamond surface plays an important role,<sup>1</sup> and the effect of different surface terminating species can greatly affect the emission characteristics.<sup>2</sup> However, since most of the results from low field emission experiments are from chemically vapor deposited (CVD) diamond with poorly characterized surfaces, it is clear that NEA is not solely responsible for the emission process. In fact there are many different mechanisms involved as the electrons travel from the negative side of the power supply, through the various interfacial contacts, through the bulk of the film itself, to the film surface, followed by field emission into the vacuum, propagate through the vacuum gap, finally reaching the collector anode. The exact nature of these mechanisms, and the way in which they interact, is still not well understood. In this work we report on the results of a series of field emission experiments performed upon undoped microcrystalline CVD diamond and amorphous DLC films produced using a variety of deposition conditions. By observing the morphology of the damaged area created by the field emission, and careful analysis of the mathematical form of the current–voltage ( $I$ – $V$ ) dependence of the emission, insight into the conduction mechanisms in the various types of film can be obtained.

The CVD diamond films were deposited onto abraded (100) Si substrates using conditions typical for a hot filament CVD reactor (process pressure 20 Torr, filament temperature 2300 °C, substrate temperature 900 °C, growth rate  $0.5\ \mu\text{m h}^{-1}$ ). Films were grown for 6 h giving a film thickness of 3  $\mu\text{m}$ . Process gas mixture was methane in  $\text{H}_2$ , with three methane concentrations. 0.5%  $\text{CH}_4$  produced high quality diamond films with few grain boundaries and crystal size around 1  $\mu\text{m}$ , 1%  $\text{CH}_4$  produced good quality diamond with more grain boundaries and crystal size around 0.5  $\mu\text{m}$ , and 2%  $\text{CH}_4$  produced poor quality “ballas” type diamond with crystal size around 0.05–0.1  $\mu\text{m}$ .

The DLC films were deposited on mirror-polished (100) Si using a 13.56 MHz radio frequency parallel plate reactor and  $\text{CH}_4$  as the sole process gas. The process pressure was varied from 5 to 200 mTorr and the rf power from 10 to 300 W (dc self-bias 60–500 V) over an 8-cm-diam electrode. The deposition time was 30 min, producing smooth, featureless DLC films of 0.1–0.2  $\mu\text{m}$  thickness. At powers greater than about 70 W, the films were hard, stressed and electrically insulating, with a high degree of  $sp^3$  character. With decreasing rf power, or increasing pressure, the films became softer and more graphitic, and were more electrically conducting.

A diode configuration consisting of a cathode (the film under test) and a tungsten tip anode (cylinder shape, 0.5 mm diameter) mounted in a turbo-pumped vacuum chamber at a base pressure of  $10^{-6}$  Torr was used to test the field emission characteristics of the films. Electrical contact was made to both the front and the back of the sample using conductive paint. The tip-sample distance was continuously adjustable to a few hundred  $\mu\text{m}$ . A negative voltage of up to 5 kV was applied to the cathode using a PC-controlled power supply, while the emission current was measured automatically as the voltage was ramped at a rate of  $\sim 50\ \text{V s}^{-1}$ . A current limit of 0.2 mA was set to avoid destruction to the films by excessive current flow. To minimize the effects of run-to-run inconsistencies, in each case  $I$ – $V$  data were measured for three films that had been deposited using identical conditions, and at two different places on each film. Values of the threshold voltage and subsequent data analysis were then calculated from an average of ten  $I$ – $V$  curves measured at each position on each sample—an average of 60 data sets in all.

During testing, it was found necessary to ramp the voltage up and down several times in order for the  $I$ – $V$  curves to stabilize and become reproducible. This conditioning effect has been reported previously,<sup>3</sup> and is accompanied by morphology changes on the film surface. These damage sites are believed to occur as a result of extremely high local fields in the vicinity of the emission site causing dielectric breakdown of the surface, followed by rapid heating and vaporization of the surface layers.<sup>4</sup> Often the presence of vapor phase spe-

<sup>a)</sup>Electronic mail: paul.may@bris.ac.uk

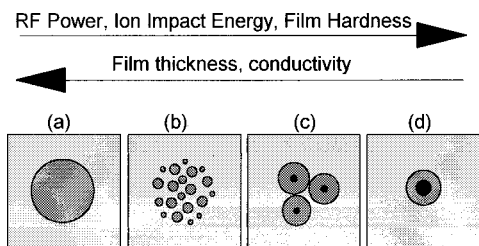


FIG. 1. Schematic diagram showing different types of damage site observed after field emission testing of DLC films grown using a range of rf powers: (a) <30 W, the DLC film has burnt off down to the Si substrate over a large area (0.5 mm diameter) corresponding to the size of the anode; (b) 30–70 W, many equally spaced craters formed; (c) 80–100W, only a few large craters, with the central section showing partial melting of the Si substrate; and (d) >100 W, a single large crater in the center of the tested area with extensive melting of the Si.

cies close to the surface, along with high fields, creates a plasma leading to a discharge, often observed as sparking between the electrodes. For the DLC films, the nature and appearance of the damaged site varied depending upon the properties of the film (see Fig. 1). Typically, a damage site would appear as in Fig. 2(a) for a DLC film deposited under medium power (for example, 50 W) conditions. A number of equally spaced holes in the film, or “craters” appear across the whole of the tested area (0.5 mm diameter). These craters were typically between a few  $\mu\text{m}$  and a few tens of  $\mu\text{m}$  in diameter, with the depth varying upon the exact testing conditions, such as the current drawn, the number of emission sites, etc. Often, the whole tested area was covered in a thin layer of graphitic material, which was presumably redeposited from the evaporated film. With prolonged testing, these craters would deepen. Raman imaging<sup>5</sup> confirmed that sometimes the craters extend several  $\mu\text{m}$  into the Si substrate, causing evaporation and redeposition of Si onto the surrounding area as well.

For DLC films produced at lower rf powers, i.e., softer, more conducting, graphitic films, the density of the craters increased, often linking up to form enlarged areas where the film no longer existed and only the Si was visible [Fig. 2(b)]. In the case of DLC films deposited at powers less than  $\sim 20$  W the crater density after field emission testing was so large that the entire 0.5-mm-diam tested area had been removed. Conversely, for films produced at high rf powers, the crater density decreased, ultimately to a single feature— either a deep crater or a hillock—located somewhere near the center of the tested area [Fig. 2(c)]. Redeposition of Si from the bottom of the crater was particularly noticeable in these harder films.

These observations can be correlated with the conductivity of the films. Graphitic films contain many conduction channels to allow passage of electrons from the contact to the surface.<sup>6</sup> Therefore we can imagine many separate emission sites turning on simultaneously when the voltage rises above a certain threshold. Space-charge effects between neighboring conduction pathways would produce an evenly distributed arrangement of channels. The current density within each channel may be high enough to cause significant local heating, leading to graphitization and subsequent evaporation of the carbon material around the channel, producing a crater. As the crater becomes deeper, even the Si substrate itself

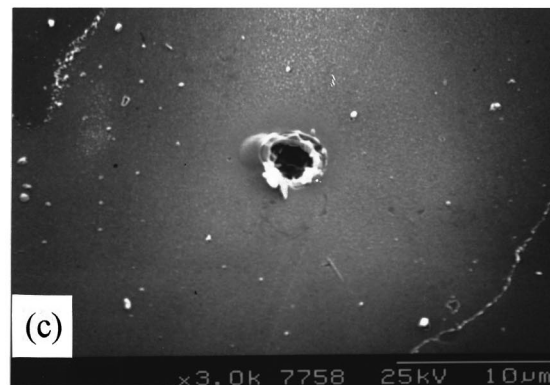
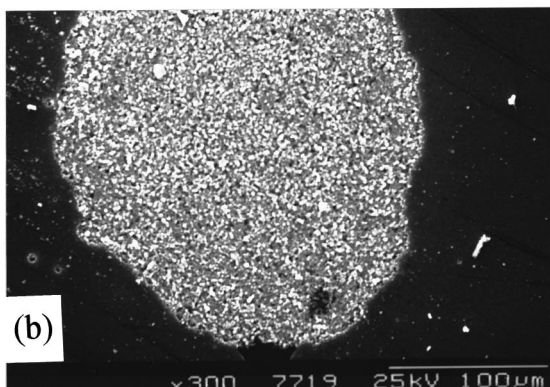
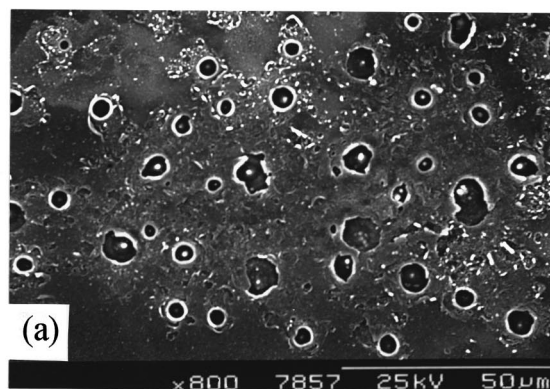


FIG. 2. Electron micrographs of the damage site from a DLC films deposited at (a) medium power 50 W, (b) low power 20 W, and (c) high power 100 W, showing the cratering behavior illustrated schematically in Fig. 1.

could melt and partially evaporate. For more insulating films, there would be far fewer conducting pathways, and as a result, a much smaller number of emission sites. Ultimately there may be only one emission site through which the entire emitted current must pass. This would lead to rapid and excessive local heating of the film and substrate, producing either a large, deep crater, or sometimes a hillock of melted and recrystallized material.

For CVD diamond films, this observed trend with conductivity is generally similar, although not as pronounced. The ballas-type films grown with high methane concentration show damaged areas containing many linked craters, whereas the more crystalline, insulating films grown with

TABLE I. The most usual mechanisms of conduction in insulators, their expected current voltage relations (see Ref. 8), and mathematical relations required for a straight line plot.

| Type of conduction   | Current–voltage relation   | Ordinate          | Abscissa   |
|--|--|-------------------|------------|
| (1) Schottky emission  | $I \sim \exp(aV^{1/2}/kT)$                                       | $\ln I$           | $\sqrt{V}$ |
| (2) Fowler–Nordheim  | $I \sim V^2 \exp(-a/V)$  | $\ln(I/V^2)$      | $1/V$      |
| (3) Space-charge limited currents (SCLC)                                       | $I \sim V$ (low fields)<br>$I \sim V^n$ ( $n > 1$ , high fields) | $I$               | $V$        |
| (4) SCLC with Poole–Frenkel (PF) effect  | $I \sim V^2 \exp(aV^{1/2}/kT)$                                   | $\ln(I/V^2)$      | $\sqrt{V}$ |
| (5) Poole–Frenkel conduction   | $I \sim V \sinh(aV^{1/2}/kT)$                                    | $\sinh^{-1}(I/V)$ | $\sqrt{V}$ |
| (6) Poole–Frenkel conduction with overlap of Coulombic potentials (Hill's law) | $I \sim \sinh(aV/kT)$  | $\sinh^{-1} I$    | $V$        |

low methane concentration show fewer isolated craters.

When discussing field emission, the most commonly used model for the ejection of electrons from a surface is the well-known Fowler–Nordheim equation.<sup>7</sup> However, this only deals with effects occurring at the surface (or at the interface between the electrical contact and the film), and there are many other models for the mechanisms of conduction in the bulk of insulators<sup>8</sup> which may be important when studying field emission from diamond. The expected current–voltage relations for some of these models are given in Table I. By plotting the appropriate mathematical form of these relations as abscissa and ordinate, a straight line plot can be obtained. The correlation coefficient of the line of best fit them gives a direct measure of how well each model fits the experimental data. Table II shows the results of the analyses for each of the CVD and DLC films investigated. For the more conducting, softer DLC films, the Fowler–Nordheim model is a better fit than the other models [except for the space charge limited current (SCLC) model which is comparable]. However, as the films become harder and more insulating, some of these other models, in particular the Schottky emission, SCLC, and SCLC with Poole–Frenkel (SCLC+PF) models, provide increasingly better fits to the data, although the Fowler–Nordheim model is still the best. However, for very insulating films (e.g., the one grown at 90 W power), these other models provide as good a fit to the data as the Fowler–Nordheim model. This trend is mirrored

in the CVD diamond films, although the data are not as clear cut: the poor quality graphitic films are best modeled with the Fowler–Nordheim equation, whereas for better quality (more diamondlike films) other models, particularly the Schottky emission, SCLC and SCLC+PF models, perform better.

A possible explanation for these observations can be made using arguments similar to those outlined above. For conducting films, the significant mechanism is probably only the tunneling of the electrons through the potential barrier, since conduction through the film should be relatively facile. For more insulating films, however, conduction through the bulk of the film could become important and potentially rate limiting. Thus, bulk conduction mechanisms (such as SCLC), as well as mechanisms occurring at the various interfaces (such as Schottky) may begin to play a significant role in the electron transport. If this is true, the observed  $I$ – $V$  dependence will then be a combination of these mechanisms and the Fowler–Nordheim surface ejection model.

An alternative mechanism, however, might involve the Si which is often evaporated from the bottom of the craters to redeposit onto the film surface. The presence of a thin Si layer covering the area immediately surrounding an emission site may affect the local emission characteristics in an unknown way. Since we observed a greater tendency for Si evaporation on the less conductive diamondlike films, it is possible that the presence of this Si coating might be responsible for the non-Fowler–Nordheim contribution to the overall emission characteristics.

TABLE II. Threshold voltages ( $V_{th}$ ) and correlation coefficients ( $r^2$ ) for the straight lines of best fit for the different data plots given in Table I and various CVD diamond and DLC films. For the PF and Hill's Law plots a straight line fit was inappropriate because the plot was obviously a curve—the  $r^2$  values for each of the films in these two models are all  $< 0.7$ , and have been omitted. To reduce scatter due to random error, the values for each film are averages from 60 sets of  $I$ – $V$  data, as described in the main text. Our estimated uncertainty in each of the quoted threshold voltages is  $\pm 4$  V, while the values for the correlation coefficients are reproducible to two decimal places.

|                          | $V_{th}/V \mu\text{m}^{-1}$ | Fowler–  |          | SCLC with |      |
|--------------------------|-----------------------------|----------|----------|-----------|------|
|                          |                             | Nordheim | Schottky | SCLC      | PF   |
| CVD 0.5% CH <sub>4</sub> | 38                          | 0.95     | 0.99     | 0.99      | 0.99 |
| CVD 1% CH <sub>4</sub>   | 25                          | 0.96     | 0.99     | 0.98      | 0.98 |
| CVD 3% CH <sub>4</sub>   | 19                          | 0.99     | 0.96     | 0.98      | 0.94 |
| DLC 30 W                 | 43                          | 0.93     | 0.90     | 0.92      | 0.85 |
| DLC 50 W                 | 31                          | 0.98     | 0.93     | 0.96      | 0.92 |
| DLC 60 W                 | 29                          | 0.98     | 0.92     | 0.96      | 0.88 |
| DLC 90 W                 | 60                          | 0.99     | 0.99     | 0.99      | 0.98 |

<sup>1</sup>C. Bandis and B.B. Pate, Appl. Phys. Lett. **69**, 366 (1996).

<sup>2</sup>P.W. May, J.C. Stone, M.N.R. Ashfold, K.R. Hallam, W.N. Wang, and N.A. Fox, Diamond Relat. Mater. (to be published).

<sup>3</sup>N.A. Fox, W.N. Wang, T.J. Davis, J.W. Steeds, and P.W. May, Appl. Phys. Lett. **71**, 1 (1997).

<sup>4</sup>R. Hessmer, M. Schreck, S. Geier, and B. Stritzker, Diamond Relat. Mater. **3**, 951 (1994).

<sup>5</sup>P.W. May, S. Höhn, W.N. Wang, and N.A. Fox, J. Appl. Phys. (submitted).

<sup>6</sup>F. Lacher, C. Wild, D. Behr, and P. Koidl, Diamond Relat. Mater. **6**, 1111 (1997).

<sup>7</sup>J.J. O'Dwyer, *The Theory of Electrical Conduction and Breakdown in Solid Dielectrics* (Clarendon, Oxford, 1973).

<sup>8</sup>P. Gonon, A. Deneuille, F. Fontaine, and E. Gheeraert, J. Appl. Phys. **78**, 6633 (1995), and references therein.